metals

MDPI

Article

The Origins of High-Entropy Alloy Contamination Induced by Mechanical Alloying and Sintering

Igor Moravcik [1,*], Antonin Kubicek [1], Larissa Moravcikova-Gouvea [1], Ondrej Adam [1], Vaclav Kana [2], Vaclav Pouchly [3], Antonin Zadera [2] and Ivo Dlouhy [1]

1 Institute of Materials Science and Engineering, Brno University of Technology, Technicka 2896/2, 61669 Brno, Czech Republic; 183435@vutbr.cz (A.K.); gouvea@fme.vutbr.cz (L.M.-G.); ondrej.adam@vutbr.cz (O.A.); dlouhy@fme.vutbr.cz (I.D.)

2 Institute of Manufacturing Technology, Brno University of Technology, Technicka 2896/2, 61669 Brno, Czech Republic; kana@fme.vutbr.cz (V.K.); zadera@fme.vutbr.cz (A.Z.)

3 CEITEC BUT, Brno University of Technology, Purkynova 123, 612 00 Brno, Czech Republic; vaclav.pouchly@ceitec.vutbr.cz

* Correspondence: igor.moravcik@vutbr.cz; Tel.: +42-911-566-030

Received: 6 August 2020; Accepted: 28 August 2020; Published: 3 September 2020

Abstract: One of the prevailing problems for materials produced by powder metallurgy is contamination from various sources. This work deals with the influence of process parameters and presence of process control agents (PCA) on the contamination level of materials produced by means of mechanical alloying (MA) technology, densified with spark plasma sintering (SPS). The equiatomic CoCrFeNi high-entropy alloy (HEA) was manufactured by the said methodology. For clear comparison, the 316L austenitic steel powder was milled and densified with identical conditions as a reference material. Both materials were milled in argon and nitrogen atmospheres for various times from 5 to 30 h. Chemical analysis of contamination by carbon, oxygen, and nitrogen within the powder and bulk materials was carried out using combustion analyzers. The microstructural analysis of powders and bulk samples was carried out using scanning electron microscopy (SEM) with focus on contaminant phases. The results show that carbon contamination increases with milling time. It is caused by wear of milling vial and balls made from high-carbon steels. Increase of carbon content within consolidation using SPS was also observed. The oxygen contamination also increases with milling time. It is more pronounced in the CoCrFeNi alloy due to higher oxidation of powder surfaces prior to milling. Milling of powders using nitrogen atmosphere also causes an increase of nitrogen content in both HEA and AISI 316L. The use of PCA (ethanol) during milling even for a short time (30 min) causes significant increase of carbon and oxygen contamination. The ways to decrease contamination are discussed in the paper.

Keywords: contamination; mechanical alloying; spark plasma sintering; infrared detection; high-entropy alloy; austenitic stainless steel

1. Introduction

Powder metallurgy (PM), as a solid-state manufacturing technique, has advantages over traditional alloying techniques—such as casting—since it permits the controlling of the microstructure during processing and mixing of insoluble phases. This leads to the production of tailored components possessing refined microstructures and enhanced mechanical properties. As such, PM is widely used for the preparation of advanced materials such as oxide dispersion strengthened (ODS) materials, and more recently, high-entropy alloys (HEAs) [1,2].

Nevertheless, one of the biggest issues concerning materials prepared by powder metallurgy is contamination, due to a significantly larger surface area of the powders compared to the surface area of

the bulk material with similar weight. Rarely, the contamination of powder materials and the resulting formation of oxides or carbides is addressed, such as the occurrence of Cr_7C_3, Cr_2O_3 and $MnCr_2O_4$ in mechanically alloyed CoCrFeNi alloy [3], where their particles have been shown to cause strengthening of the alloy, but decrease in ductility. Moreover, the contamination may be used as an efficient feedstock alternative on the production of ODS alloys, since PM procedures enable homogeneous distribution of oxides and/or carbides into a metal matrix. As such, the nanograined modified oxides in ODS materials contribute to the overall strengthening of the material while maintaining satisfactory ductility [4].

Consequently, the presence of oxides and carbides formed in the resulting microstructure can have a significant influence on the properties of the final materials [5]. Furthermore, these particles lower the amount of important alloying elements such as Cr in a surrounding solid solution and thus may lead to loss of corrosion resistance [6].

That said, it is important to emphasize that it is very difficult to control the contamination level of the powders during mechanical alloying, as it is an inherent characteristic of the PM process. Thus, its complete avoidance becomes challenging.

The contamination, however, can be greatly limited by controlling and optimizing the parameters of its possible sources. It has been previously reported that the main sources of contamination of PM are storage and transfer of powders, milling equipment, milling atmosphere, and the use of process controlling agents (PCA) [7].

Powder metallurgy has been frequently studied as a suitable technique to produce high-entropy alloys [4,8–12]—a relatively new class of multicomponent alloys with near equiatomic compositions [13,14]. Some of these HEAs have exhibited outstanding mechanical properties in a range of temperatures from cryogenic [15] to very high working temperatures [16], such as mutually high strength and ductility [17–19] and remarkable fracture resistance [20].

In this light, the present work aims on elucidating the evolution of the contamination level on PM-produced high-entropy alloy powders in comparison with traditional 316L steel powders. More specifically, the CoCrFeNi composition was chosen due to its remarkable mechanical properties when prepared by PM [3,21]. A systematic characterization of powders at different times of milling and atmospheres was performed, especially regarding the increase of the amounts of oxygen, nitrogen, and carbon in each alloy.

2. Materials and Methods

Equiatomic, high-entropy alloy powders with chemical composition of CoCrFeNi (ratio of 1:1:1:1) were prepared by mechanical alloying (MA) followed by spark plasma sintering (SPS).

The CoCrFeNi alloy powders were prepared from pure elemental powders, whereas the information on the powders' characteristics are given in Tables 1 and 2. For reference, the 316 L alloy atomized powder was also milled with the same parameters. The powders were milled using a 10:1 ball-to-powder weight ratio, with 10 mm diameter balls. Each starting powder mixture weighed 30 g. Milling balls and powder mixtures were introduced into a high-carbon steel hardened steel milling container. The milling container was then sealed and flushed with Ar or N_2 gas (purity 99.998%) to limit powder oxidation during the milling process. Dry milling was performed in Pulverisette 6 ball mill (Fritsch GmbH, Germany) with a milling rate (ratational) of 300 rounds per minute. The total milling time was selected from 5–50 h for different millings. In the end of the dry-milling process, the free powders were removed from the milling bowl and stored under protective atmosphere. The scheme of the parameters pertaining to powder material preparation is presented in Figure 1.

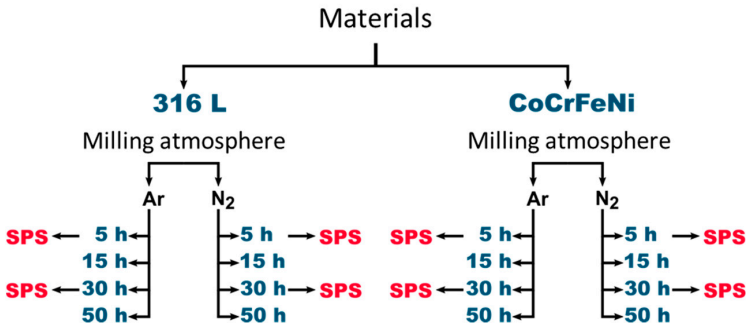

Figure 1. Schematic representation of various powder materials prepared using a set of variable milling parameters (time, atmosphere). The 316 L alloy atomized powder and CoCrFeNi powder prepared from pure elements was used for milling experiments. Powder samples designated by the spark plasma sintering (SPS) arrow were subsequently densified.

Additionally, empty bowls still containing part of the powders in the form of an adhesive layer stuck to its walls (Figure 2) were filled with 200 mL of ethanol and wet-milled for 30 min. This was done to fully remove the powders stuck to the milling equipment. The extracted powders were then filtered and dried. The wet-milled powders were measured separately only to evaluate the concentration of C, N, and O. This measurement was performed to evaluate the level of contamination caused by wet milling, compared to dry-milled powders.

The "0 h of milling" condition represents the unmilled alloys, i.e., the ones that simply were not subjected to the MA process. Instead, the input powders Co, Cr, Fe, and Ni were manually mixed in an equiatomic ratio, before being inserted into the milling bowl.

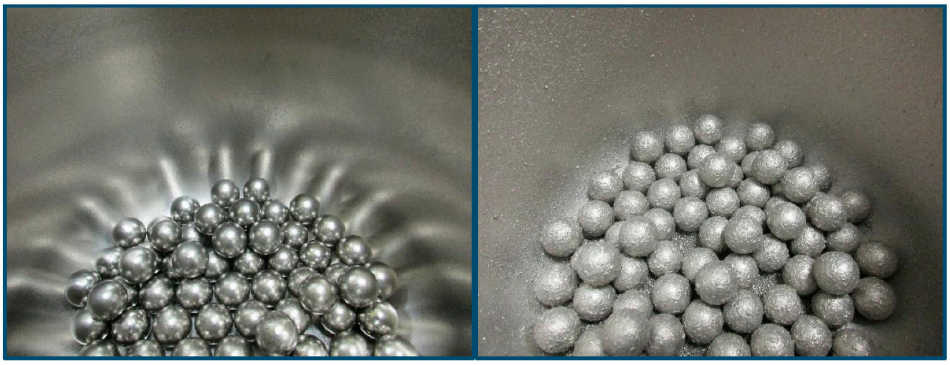

Figure 2. Inside of the milling bowl before (**left**) and after (**right**) the dry milling process of the CoCrFeNi powders milled for 15 h. Apart from the free powder at the bottom, the inside of the bowl still contains significant amount of powder stuck to its walls and to the milling balls, which were removed by 30 min of wet milling.

Table 1. Manufacturers and product parameters of powders used for preparation of mechanically alloyed CoCrFeNi alloy.

Element	Manufacturer	Product Identification
Co	Alfa Aesar	Particle size < 44 μm, purity 99.5%
Cr	Alfa Aesar	Particle size < 44 μm, purity 99%
Fe	Alfa Aesar	Particle size < 10 μm, purity ≥ 99.5%
Ni	GTV	Particle size 15–53 μm, purity 99%
316L	Höganäs AB	53–150 μm, purity 99.5%

Table 2. Chemical composition and of 316L alloy powder from Table 1.

Element	Fe	C	Mo	Ni	Mn	Cr	Si	O
wt.%	65.83	0.014	2.4	12.3	1.6	17.0	0.8	0.059

MA powders were subsequently sintered by SPS dr. Sinter SPS625 in a 12-mm-diameter graphite die using a graphite foil interlayer between the powder and die to ensure proper electrical contact. The amount of used powders was calculated to obtain 5-mm-thick cylindrical samples. The sintering was performed from room temperature with a heating rate of 100 °C/min till final temperature of 900 °C with a dwell of 10 min and uniaxial pressure of 50 MPa in vacuum atmosphere. At the end of sintering, the setup was left to naturally cool down, until it was opened at ~200 °C. Sintered samples were then cut and prepared by standard metallographic procedures. The porosity, as well as particle size and area, were measured using ImageJ software on micrographs taken by scanning electron microscope (SEM). ULTRA PLUS (Carl Zeiss GmbH, Germany) with the Energy-dispersive X-ray spectroscopy (EDS) detector were utilized for analysis of powder and bulk microstructures and chemical composition determination. The exact concentrations of C element were measured in the milled powders and bulk materials using combustion analyzers G4 ICARUS (Bruker, Billerica, Massachusetts, MA, USA), whereas O and N were measured using an TC-336 analyzer (LECO Corporation, St. Joseph, Michigan, MI, USA).

3. Results

3.1. Carbon Contamination of Powders

Figure 3 depicts the increase of carbon concentration in the milled powders, as a function of the milling time. The carbon concentration of 0.023 ± 0.001 wt.% represents impurities present in the unmilled powders, i.e., 0 h of milling—please refer to the previous section for more details. It is evident that regardless of used atmospheres (Ar or N_2) the concentration of carbon increases continuously with the increase of the dry-milling time in both alloys. The extent of carbon contamination at the same milling times in 316 L steel is slightly larger than in the HEA. The differences in used atmosphere do not significantly change the contamination either. However, the dashed line in Figure 3a shows that the carbon contamination further increases by 0.05–0.1 wt.% by additional milling in carbon based PCA (ethanol). Such high levels of contamination as, for instance, 0.340 ± 0.005 wt.% of carbon in HEA milled for 30 h in Ar and 30 min in ethanol should result in significant changes of alloy powder chemistry and properties, as discussed later. The only source of carbon available during dry milling is the high-carbon steel, from which milling equipment (bowl and balls) is made. Therefore, the carbon contamination is a consequence pertaining to the wear of milling equipment.

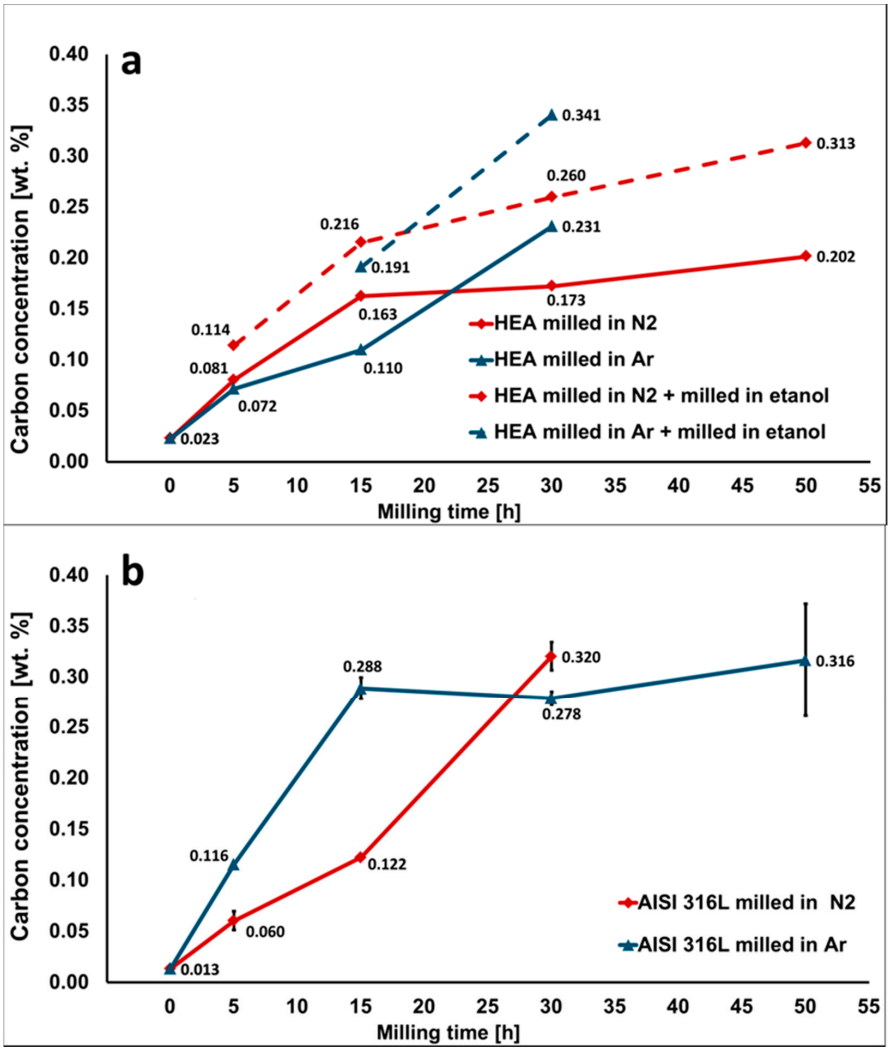

Figure 3. Carbon concentration of powders milled in Ar and N_2 atmosphere as a function of the milling time: (**a**) high-entropy alloy (HEA) powder, the dashed line represents powders additionally milled in process control agents (PCA) (ethanol) for 30 min; and (**b**) 316 L steel powder. The carbon contamination caused by the wear of high-carbon steel milling equipment is increasing with milling time.

3.2. Carbon Contamination during SPS

The next step in the preparation of the bulk samples from powder is SPS densification. In this process, the powder is placed in a graphite die and subsequently uniaxially pressed, while being simultaneously heated at the same time. Figure 4 shows significant increase of the carbon concentration after SPS, compared to milled powders of both alloys. The data show that powders milled for shorter times (5 h) show lower increase of carbon concentration after SPS, compared to powders milled at longer time (30 h). Since increase of carbon content after SPS is probably caused by diffusion of carbon from a carbon-rich environment in the SPS die into the bulks, the higher number of lattice defects (mediators of diffusion) in powder milled for longer times can be caused by enhanced diffusion rate.

It is interesting to remark that the 316 L steel on average seems to absorb more carbon from the SPS carbon-rich environment than the HEA. This can be caused by different solubility of carbon in 316 L steel, compared to HEA. However, it should be noted that the values of carbon contents given for bulk samples do not perfectly represent mean values of contents. Within a small volume of sintered samples, it was possible to perform only one measurement. The values of the contents of the elements

in bulk samples should therefore be taken as indicative only, serving mainly to visualize the trend of changes that have taken place within the SPS process.

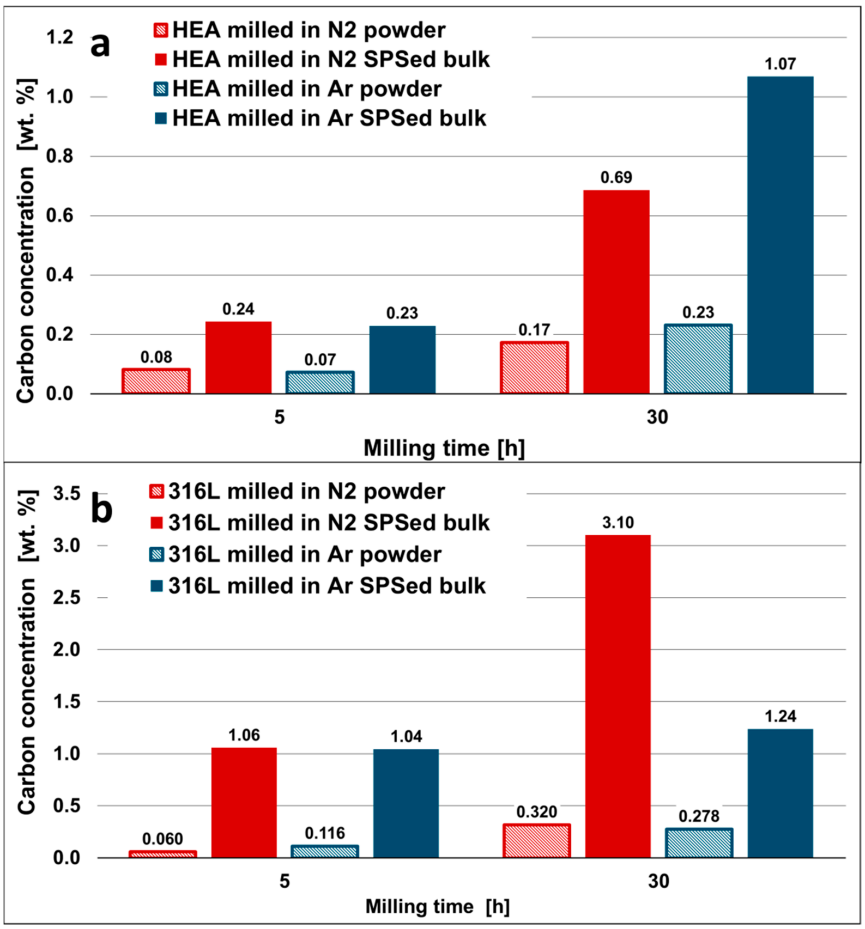

Figure 4. Carbon concentration of selected powders milled in Ar and N_2 atmosphere as compared to concentration of the same materials after the SPS process (SPSed bulks); (**a**) HEA and (**b**) 316 steel. The SPS densification in graphite die significantly increases carbon contamination.

3.3. Oxygen Contamination of Powder

The increase of oxygen concentration in the milled HEA powders as a function of milling time is shown in Figure 5a. The oxygen content in the initial condition (unmilled powders) was in a concentration of 0.398 ± 0.003 wt.%. After 5 h of dry milling, it is evident that there is a substantial increase in the oxygen concentration independent of the chosen atmosphere (Ar or N_2), which clearly evidences that the contamination is not influenced by the used protective atmosphere; however, the contamination is most pronounced at this stage.

After 5 h of dry milling, the oxygen contents for all conditions do not vary significantly. Even reaching 15 h of dry milling, the oxygen concentration keeps steady and does not suffer any significant changes, considering the data scattering. After 15 h of dry milling, the MA route is divided within wet (dashed line) and dry milling (full line). Dry milling clearly does not provide any important increase in the oxygen content, even up to 50 h, regardless of the atmosphere, at which the difference goes from 0.517 ± 0.061 wt.%. (for 5 h) up to a maximum of 0.589 ± 0.032 wt.% (for 50 h).

Additional wet milling (30 min in ethanol) was performed after 15, 30, and 50 h of dry milling. It is clear that for the same total milling time, the dry milling possesses a much lower oxygen concentration using both atmospheres, e.g., HEA milled for 15 h in N_2 (0.458 ± 0.065 wt.%), compared to HEA milled for 15 h in N_2 and ethanol (0.600 ± 0.070 wt.%).

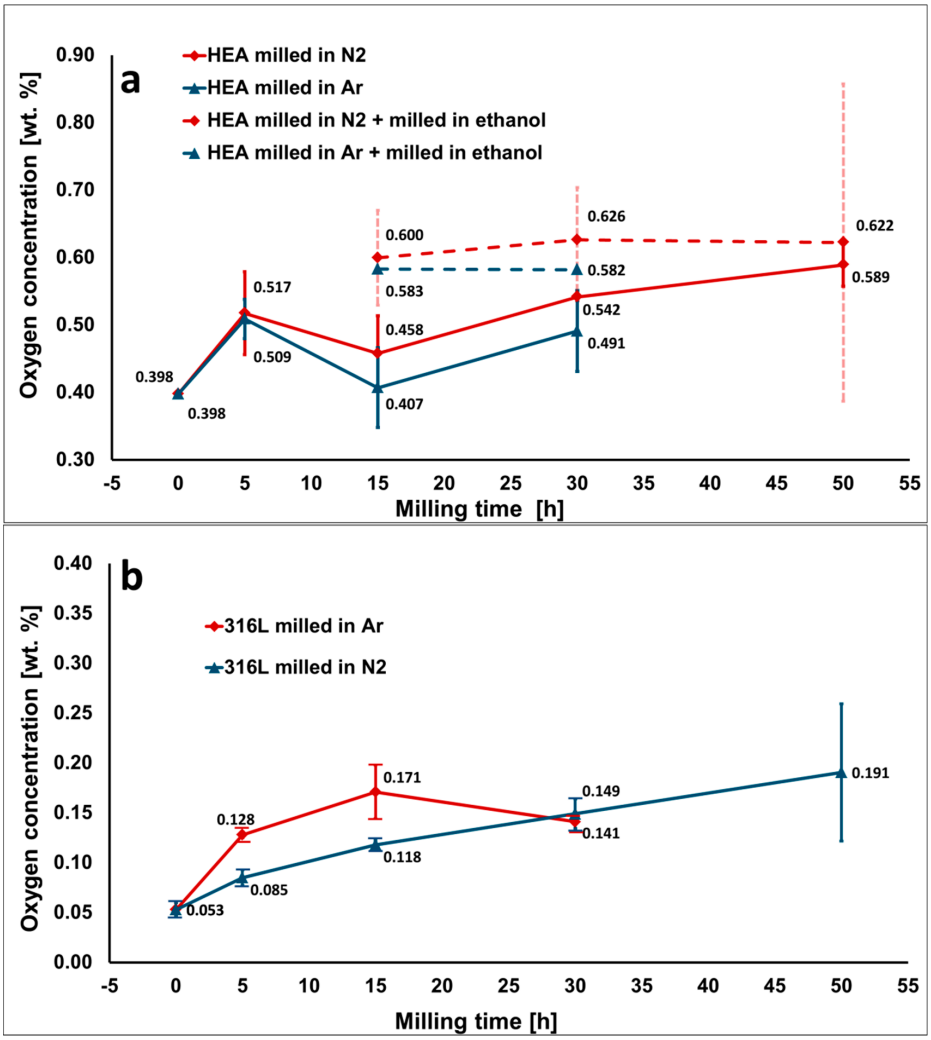

Figure 5. Oxygen concentration of the powders milled in Ar and N_2 atmosphere as a function of the milling time: (**a**) HEA powder, the dashed line represents powders additionally milled in PCA (ethanol) for 30 min; and (**b**) 316 L steel powder. The oxygen contamination gradually increases with milling time. Relatively high-oxygen concentration in unmilled HEA powder (0 h) is caused by initial oxidation of surfaces of elemental pure powders prior to milling.

The wet milling shows a weak dependence on the used atmosphere. When Ar is used allied with ethanol as PCA, from 15 h up to 30 h of milling, the oxygen level is steady and shows no increase in absolute numbers. When N_2 is used, there is a slight rise in oxygen concentration from 0.600 ± 0.070 wt.%. up to 0.626 ± 0.078 wt.%.

Figure 5b shows the oxygen concentration as a function of milling time for 316 L steel powders. Both atmospheres of choice provide the same total contamination level up to 30 h of dry milling, from 0.053 ± 0.007 up to 0.149 ± 0.015 wt.% in oxygen concentration. After 50 h of milling, there is a substantial increase in the oxygen concentration to 0.191 ± 0.069 wt.%.

The protective atmosphere does not seem to have significant influence on the amount of oxygen during milling for both powders overall globally considering the small differences, but the milling in Ar resulted in slightly lower oxygen contamination. Wet milling appears to play a more important role in the oxygen concentration, with a consistent increase in the amount of oxygen, which will be further explained in the Discussion section.

3.4. Nitrogen Contamination of Powders

Figure 6 displays the increase of nitrogen concentration in the milled powders, as a function of the milling time. As was expected, N_2 atmosphere has a more pronounced effect on nitrogen contamination than Ar atmosphere, since N_2 atmosphere is not inert and nitrogen can be dissolved in both alloys. A significant difference in nitrogen concentration of unmilled powders of HEA and 316 L steel has been noted (0.008 ± 0.001 wt.% and 0.065 ± 0.002 wt.%, respectively). In the case of HEA milled in N_2 atmosphere, it is evident that after 5 h of dry milling, there is a considerable increase in nitrogen concentration to 0.051 ± 0.006 wt.% (Figure 6a). From 5 h onwards, the nitrogen content is slowly increased with the increase of the dry-milling time and the values of contamination are comparable with 316 L steel milled in N_2. Ar atmosphere has almost no effect, and the nitrogen content of milled powders remains similar to the unmilled powders. Additional milling in ethanol (dashed line) does not cause any changes in the contamination level in both atmospheres. The increase after 50 h of milling is questionable because of the high-data scattering.

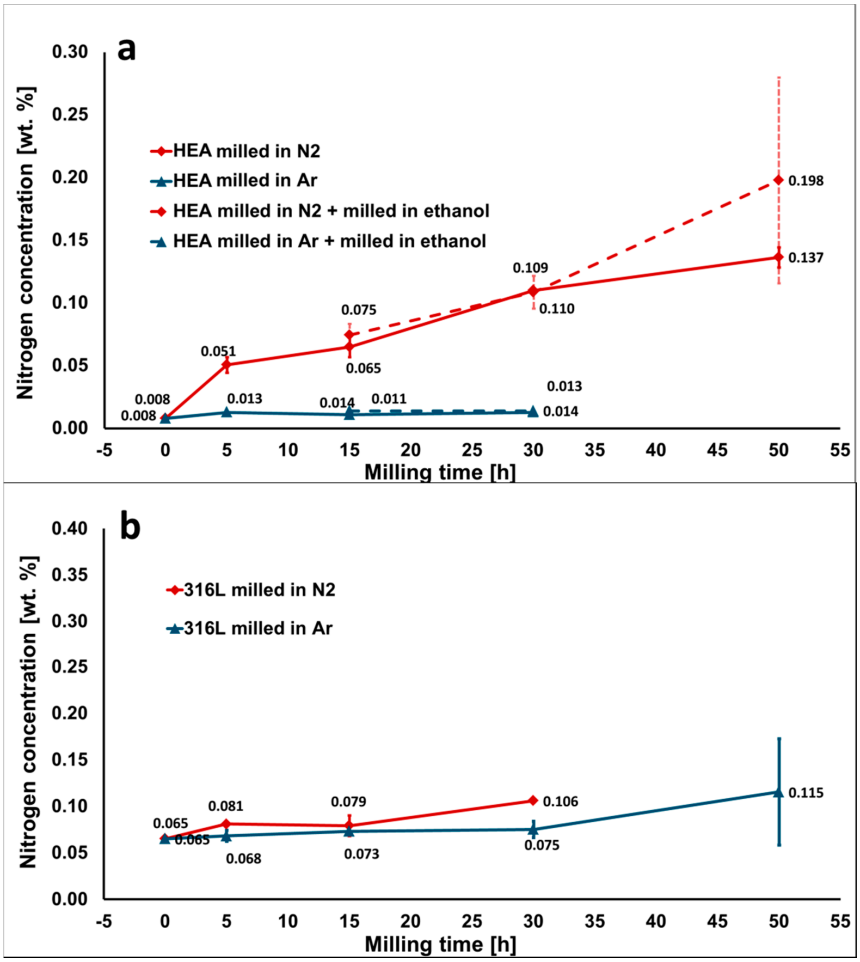

Figure 6. Nitrogen concentration of powders milled in Ar and N_2 atmosphere as a function of the milling time: (**a**) HEA powder, the dashed line represents powders additionally milled in PCA (ethanol) for 30 min; and (**b**) 316 L steel powder. The milling in Ar atmosphere prevents nitrogen contamination, while milling of the HEA powders in N_2 atmosphere causes significant nitrogen pick-up.

3.5. Oxygen and Nitrogen Contamination of the Bulks

The values in Figure 7a show the variation in concentrations of oxygen after the 5 h-milled HEA powders were consolidated into bulks using SPS. The concentrations of oxygen in the bulks remain

without statistically significant deviation from the powder ones. The measurements for other milling times (not shown here) exhibited the same trend. Therefore, the initial concentration of oxygen does not change during consolidation, despite the use of reduction atmosphere (vacuum + C rich gases) during SPS. This may be associated with high stability of the oxides. However, there were instances when the oxygen concentration slightly decreased after SPS.

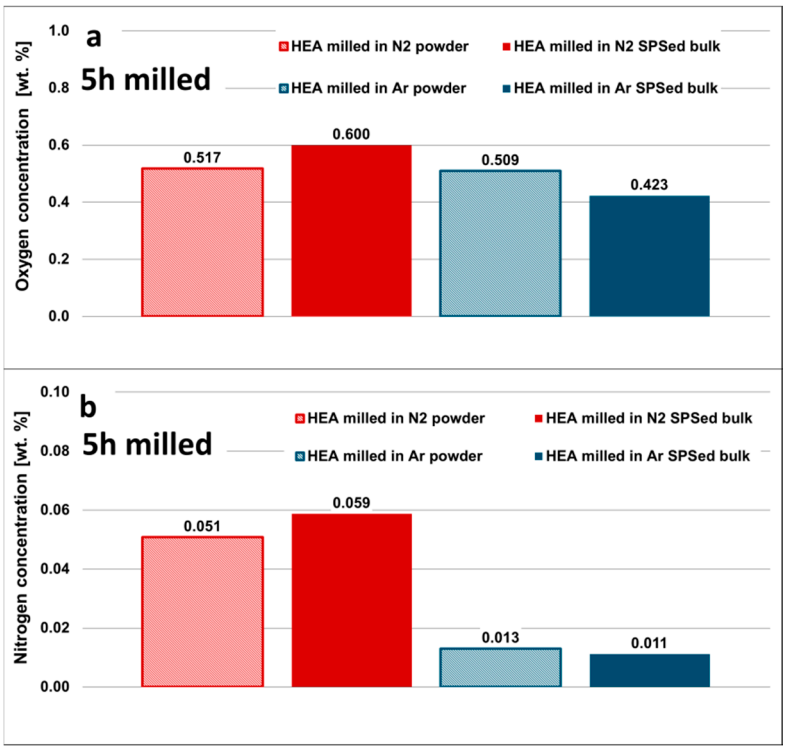

Figure 7. Comparison between the powder and bulk materials of HEA milled for 5 h in Ar and N_2 atmosphere; (**a**) oxygen concentration and (**b**) nitrogen concentration. The nitrogen and oxygen concentrations are retained after the SPS, within the scatter of the measurements and their accuracy.

In the same manner as oxygen, nitrogen concentration (Figure 7b) inside the bulks remains statistically consistent with the nitrogen concentration inside powders from which the bulks were prepared.

3.6. Microstructure of the Bulks

The representative microstructures of bulk materials with EDS spectrums of each phase in CoCrFeNi and 316 L steel are shown in Figure 8a,c and Figure 8b,d respectively. The bulk samples were sintered from powders milled in Ar atmosphere for 30 h. The microstructures of both samples are very similar, consisting of a face centered cubic (FCC) matrix and two types of particles homogeneously dispersed within the matrix. At some areas (marked by green rectangle in Figure 8), the particle size is extremely small, in the range of tens of nanometers. According to EDS analysis, the larger particles are Cr carbides (marked by yellow arrows) that are a result of carbon contamination during milling. Additionally, the round-shaped particles (denoted by red arrows) were determined to be oxides, more specifically, Cr oxides for the HEA and complex (Mn, Si) oxides for the 316 L steel. It should be noted that due to the inherent insensitivity of EDS to light elements, the exact quantities of C and O elements in the tables embedded in Figure 8c,d are pre-sented only for informative purposes, and they may deviate from the real concentrations. The reason for their presentation is to clearly show the C– or O– rich nature of particles within the microstructure, identified as carbides and oxides, respectively.

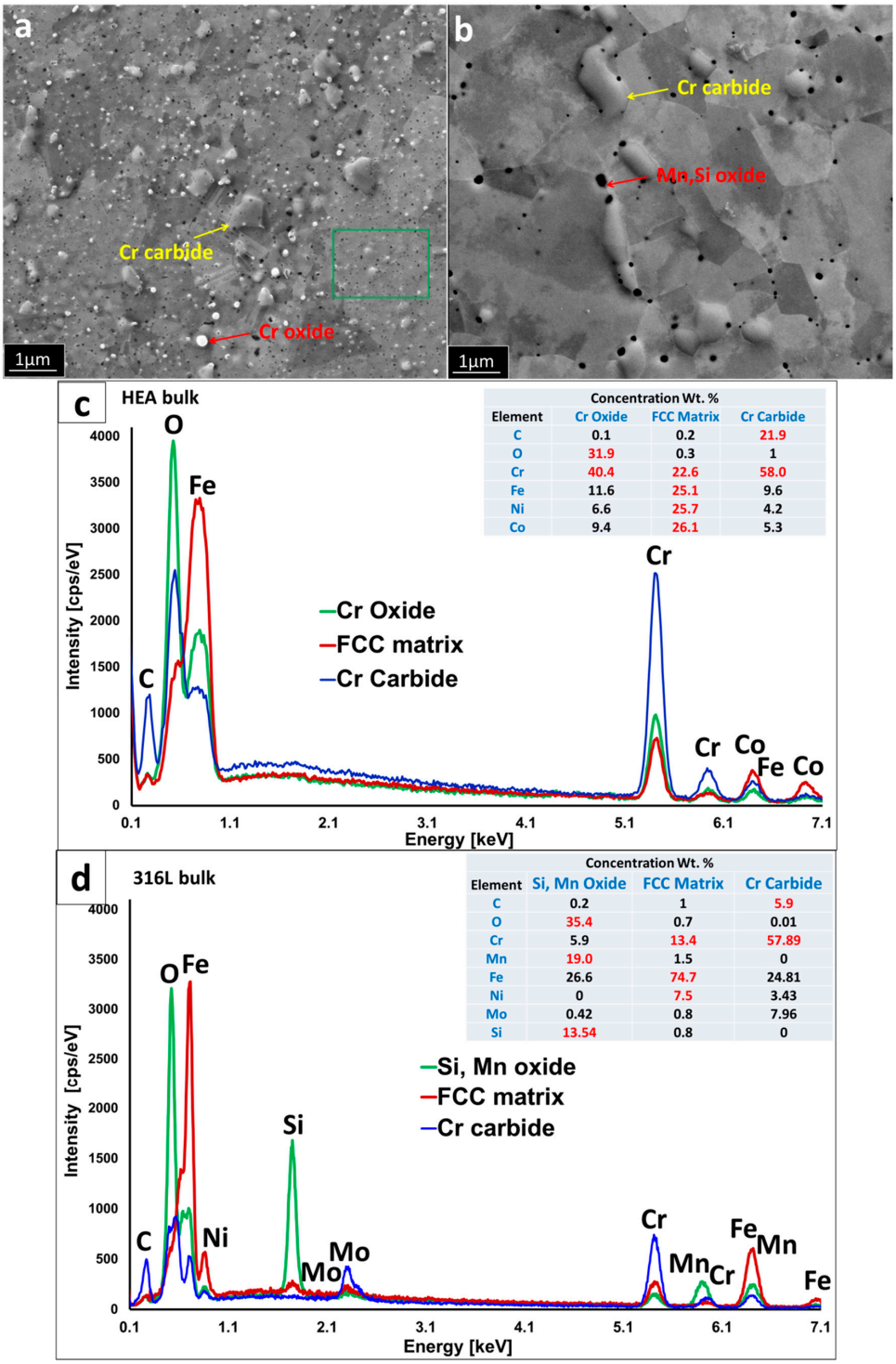

Figure 8. Representative microstructures of the bulk materials prepared from powders milled in Ar atmosphere for 30 h, taken with SEM in secondary electrons mode; (**a**) HEA; (**b**) 316L steel; (**c**) EDS analysis of representative particles in HEA; and (**d**) EDS analysis of representative particles in 316 L steel. The microstructures are composed from FCC matrix grains, oxide particles with varying chemistry and size, and larger chromium carbide particles. It should be noted that due to the insensitivity of EDS to light elements, the exact quantities of C and O elements presented in tables are only for informative purposes.

These particles may induce significant strengthening effect to the materials, as already quantified by the authors for similar alloys [4,17,22].

4. Discussion

To summarize the effects of milling and SPS densification on carbon, oxygen, and nitrogen contamination of the materials, the results for the CoCrFeNi HEA sample milled for 30 h in N_2 atmosphere are shown in Figure 9.

Regarding the role of the PCA during processing, the results showed that even a short wet milling continuing for only 30 min in ethanol (C_2H_5OH) contributes to significant contamination of powders by oxygen and, to a larger extent, by carbon. We may speculate that the use of oxygen-free PCA, such as toluene, could decrease the oxygen contamination, but it would still lead to carbon contamination [23]. Therefore, it is advisable to completely avoid using PCA during milling.

Oxygen causes the most significant contamination in the unmilled powders. At the respective concentrations measured inside the produced HEA materials (up to ~0.5 wt.%), oxygen contamination can induce significant changes of properties and microstructures. Oxygen is already present on the surfaces of raw powders in the form of various oxides. The oxides form due to reaction of metallic surfaces with ambient air. The layer of oxides is formed on the surfaces of metals already during powder manufacturing and can grow during the storage [24]. Elements with relatively high affinity for oxygen, such as chromium and iron in our case, are very prone to oxidation [25]. This pre-processing oxidation of the raw elemental powders is one of the most significant contributions to the contamination of the final bulks. It should be noted that suppression of contamination during elemental powder preparation is extremely difficult. In some cases, it can be induced by selection of specialized methods, such as vacuum atomization and powder handling under protective atmospheres [26]. The oxygen contamination slightly increases also after milling for 30 h, even despite the use of protective N_2 atmosphere (Section 3.3). The contamination can be explained by the leak of air, due to their not being a 100% air tighten milling bowl. However, a more probable explanation is the impurities contained in the N_2 gas, where some of the remaining oxygen is always presented. The new surfaces created by milling are then immediately oxidized by oxygen impurities inside the bowl, as well as during opening of the milling bowl at the end of milling and feeding the powder to the SPS die. The densification inside SPS either retains the oxygen concentration of the milled powders, or it can slightly decrease it. The slight oxygen decrease observed in some cases can be rationalized on the basis of the nature of sintering environment (slight reducing atmosphere of vacuum and C-rich gasses), combined with relatively high processing temperature. The latter setup could result in a tendency to degas the powders, comparable to degassing by use of vacuum during melting (VIM and VAM process). The use of high-vacuum during the SPS process could also decrease the extent of oxygen contamination in the materials with low affinity to it.

Carbon contamination is even more problematic than oxygen. The initially mixed powders contain a relatively low concentration of carbon. However, even such a low concentration of carbon can cause issues for materials prone to sensitization [27]. The carbon contamination is considerably increased by the milling process, positively increasing with prolonging milling time. Such carbon concentration is tenths of wt.% and would significantly alter the properties of FCC HEAs [22], by formation of carbides and interactions inside a matrix solid solution. Carbon contamination during milling is caused by the abrasive wear of the milling bowl and balls, made from hardened high-carbon steel. This type of contamination will be observed in various types of milling equipment, because hardened steel (bearing steel, tool steel, etc.) is the most common material used for the milling bowl [7,28]. The use of steel equipment also results in contamination by iron [29]. On the other hand, iron contamination levels during milling are not significant in cases of iron-containing materials, such as the CoCrNiFe HEA. The contamination from the milling equipment has been observed in all types of materials prepared with milling equipment made from metals and ceramics such as, for instance, WC [23], SiC [30], and stainless steel [31]. The general rule to eliminate said contamination induced by equipment

abrasion is to reduce the milling time to the largest possible extent. The best way to completely eliminate the contamination of the powders from the milling equipment would be to use the equipment (milling balls and bowl) made from the material identical to that which is being milled. However, this option will be possible only in very limited number of cases due to the sheer variety of milled materials and, on the other hand, limited amount of materials used for the milling equipment. Finally, the largest contamination by carbon results from graphite die-processed powder interaction in SPS. Such contamination has been documented before [32]. However, it is not clear if the contamination is caused by the reaction of the powders in the direct vicinity of graphite mold, or if it is carried by a carbon-containing gas emanating during SPS. The carbon contamination from the graphite die can be reduced by application of protective coating on the die walls in the form of spray (BN powder) or use of different die materials (tungsten). Additionally, the layer of protective material can be added in some cases in the form of thin sheet (steel, Nb), preventing the direct contact of the powder with the graphite die.

The least significant contribution to overall contamination is caused by nitrogen. The nitrogen contamination of the initial powders is very low. Additionally, the utilization of Ar inert gas during milling secures stable values of nitrogen concentration throughout the whole processing. In case the nitrogen level has to be decreased further, the use of high-vacuum during the SPS process could decrease nitrogen contamination even further.

One of the most significant observations of the study comes from the comparison between preparation by milling from elemental powders (CoCrFeNi HEA) and milling of pre-alloyed powder (316L steel). It is evident that the use of pre-alloyed gas atomized powder results in significantly purer materials, when compared to preparation from mixed elemental powders with desired composition. This is caused by lower initial contamination of pre-alloyed powder (especially by oxygen), resulting in consistently less contaminated materials prepared from pre-alloyed powders.

There are slight differences between the extent of contamination of the 316 L steel and the HEA caused during milling, presumably caused by the differences in the chemical composition. The largest difference is visible in more significant increase of carbon concentration of 316 L steel during milling and subsequent sintering. It can be explained by the chemical composition of the 316 L steel, containing larger concentration of Fe. The HEA shows lower affinity towards carbon, due to lower content of Fe and higher content of Ni and Co, i.e., elements with lower affinity for carbon (less negative enthalpy of mixing of Ni and Co compared to Fe [33]). As mentioned previously, the differences in the total concentrations of oxygen and nitrogen in the 316 L steel and HEA are mostly caused by the differences in their initial content in used raw materials. However, the extent of contamination caused during preparation is comparable in both materials.

In conclusion, the use of inert-gas atomized, pre-alloyed powder handled in protective atmosphere, avoidance of PCA, and minimization of mechanical milling time results in minimal contamination of the final bulks. In special cases, the use of an SPS die treated by protective layers (BN) and utilization of high-vacuum during sintering could be also beneficial. The preparation of alloy powder by mechanical milling of elemental powders produces more contaminated bulks, compared to preparation from atomized powders. On the other hand, the use of elemental powders offers a better versatility and timeliness for preparation of various arrays of materials, compared to atomization. For the atomization, the desired material has to be prepared in the form of ingot prior to atomization, complicating the processing. Therefore, preparation of powders by milling (alloying) of elemental powders is the process of choice for instances when shorter time for preparation of final bulk outweighs the issues of contamination, such as initial alloy screening.

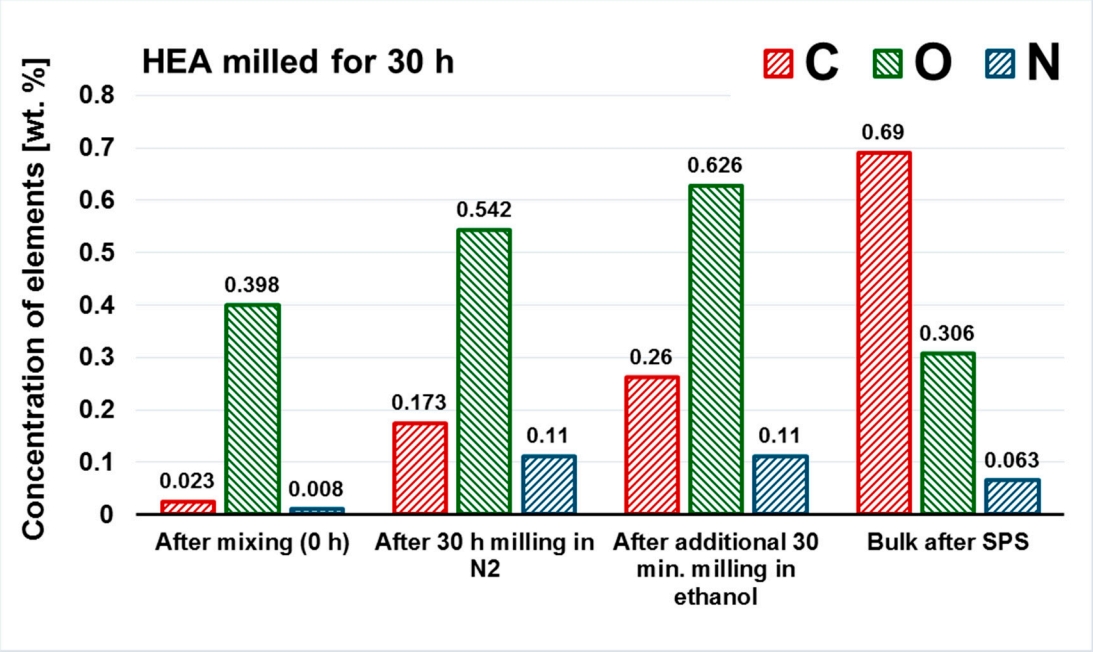

Figure 9. The evolution of contamination in the representative case of HEA powder milled for 30 h and additional 30 min in ethanol. The SPSed bulk was prepared from the powder after 30 h of milling.

5. Conclusions

In this study, the CoCrFeNi high-entropy alloy (HEA) powder and bulk forms were subject to a systematic chemistry analysis in order to evaluate the extent of contamination at every single stage of the powder metallurgy production process. For comparison purposes, the same procedure was performed in a 316 L stainless steel material. The powders were mechanically alloyed and subsequently spark plasma sintered (SPS). The influence of milling times, selected protective atmosphere during milling (Ar or N_2), use of PCA, and sintering process were discussed in terms of oxygen, nitrogen, and carbon contents. The main outcomes of this investigation can be summarized as follows.

Abrasion of the high-carbon steel milling bowl and balls has been identified as a significant source of contamination of powder materials in the mechanical alloying (MA) process. Due to the increased carbon contents, a considerable amount of carbides was observed in the structures of both HEA and steel samples. These inclusions can significantly affect the mechanical, corrosion and other properties of the final products.

The most significant contamination by oxygen is induced by the initial oxidation of raw powder surfaces. Oxygen contamination also slightly increases with milling time.

In the case of the HEA prepared from elemental powder, the oxygen contamination caused by oxidation of raw powder before milling induces formation of significant volume of oxides in the sintered bulks.

The bulk of Cr-containing alloy (HEA) prepared using pure elemental powders shows significantly higher oxygen contamination than bulks prepared from pre-alloyed powder (316 L steel).

The protective atmosphere does not seem to play an important role in the amount of oxygen and carbon contents during milling, even though the use of Ar resulted in slightly lower oxygen contamination.

The nitrogen contamination is significantly higher when using N_2 atmosphere, compared to use of Ar.

Wet milling in 200 mL of ethanol led to an increase in carbon and oxygen contents of all samples as compared to dry milling.

The significant contribution to the overall carbon contamination of the bulk materials is also caused by the SPS process, as the powders possibly react with the carbon-rich environment inside the graphite die, substantially increasing the carbon levels of the sintered bulk products.

Author Contributions: Conceptualization: I.M., A.K., and I.D.; methodology: I.M., A.K., and V.K.; validation: I.M., A.K., and V.K.; formal analysis: I.M., A.K., L.M.-G., and O.A.; investigation: I.M. and A.K.; resources: V.P., A.Z., and I.D.; data curation: I.M., A.K., and V.K.; writing—original draft preparation: I.M., A.K., L.M.-G., and O.A.; writing—review and editing: I.M., L.M.-G., and O.A.; visualization: I.M., A.K., L.M.-G., and O.A.; supervision: I.M. and I.D.; project administration: I.M. and I.D.; funding acquisition: I.D. All authors have read and agreed to the published version of the manuscript.

Funding: This research was funded by the Czech Science Foundation Project No. 19–22016S and the project ArMADit no. CZ.02.1.01/0.0/0.0/16_025/0007304.

Acknowledgments: This work was financially supported by Czech Science Foundation Project No. 19–22016S and the project ArMADit no. CZ.02.1.01/0.0/0.0/16_025/0007304.

Conflicts of Interest: The authors declare no conflict of interest.

References

1. Moravcikova-Gouvea, L.; Moravcik, I.; Omasta, M.; Veselý, J.; Cizek, J.; Minárik, P.; Cupera, J.; Záděra, A.; Jan, V.; Dlouhy, I. High-strength Al0.2Co1.5CrFeNi1.5Ti high-entropy alloy produced by powder metallurgy and casting: A comparison of microstructures, mechanical and tribological properties. *Mater. Charact.* **2020**, *159*, 110046. [CrossRef]
2. Moravcik, I.; Gamanov, S.; Moravcikova-Gouvea, L.; Kovacova, Z.; Kitzmantel, M.; Neubauer, E.; Dlouhy, I. Influence of Ti on the Tensile Properties of the High-Strength Powder Metallurgy High Entropy Alloys. *Materials* **2020**, *13*, 578. [CrossRef] [PubMed]
3. Li, M.; Guo, Y.; Wang, H.; Shan, J.; Chang, Y. Microstructures and mechanical properties of oxide dispersion strengthened CoCrFeNi high-entropy alloy produced by mechanical alloying and spark plasma sintering. *Intermetallics* **2020**, *123*, 106819. [CrossRef]
4. Moravcik, I.; Gouvea, L.; Hornik, V.; Kovacova, Z.; Kitzmantel, M.; Neubauer, E.; Dlouhy, I. Synergic strengthening by oxide and coherent precipitate dispersions in high-entropy alloy prepared by powder metallurgy. *Scr. Mater.* **2018**, *157*, 24–29. [CrossRef]
5. Guo, L.; Ou, X.; Ni, S.; Liu, Y.; Song, M. Effects of carbon on the microstructures and mechanical properties of FeCoCrNiMn high entropy alloys. *Mater. Sci. Eng. A* **2019**, *746*, 356–362. [CrossRef]
6. Abbaschian, R.; Abbaschian, L.; Reed-Hill, R.E. *Physical Metallurgy Principles*, 4th ed.; Cengage Learning: Stamford, CT, USA, 2008; ISBN1 10: 0495082546, ISBN2 13: 9780495082545.
7. Suryanarayana, C. Mechanical alloying and milling. *Prog. Mater. Sci.* **2001**, *46*, 1–184. [CrossRef]
8. Moravcik, I.; Cizek, J.; Zapletal, J.; Kovacova, Z.; Vesely, J.; Minarik, P.; Kitzmantel, M.; Neubauer, E.; Dlouhy, I. Microstructure and mechanical properties of Ni1,5Co1,5CrFeTi0,5 high entropy alloy fabricated by mechanical alloying and spark plasma sintering. *Mater. Des.* **2017**, *119*, 141–150. [CrossRef]
9. Moravcik, I.; Gouvea, L.; Cupera, J.; Dlouhy, I. Preparation and properties of medium entropy CoCrNi/boride metal matrix composite. *J. Alloys Compd.* **2018**, *748*, 979–988. [CrossRef]
10. Gouvea, L.; Moravcik, I.; Cizek, J.; Krajnakova, P.; Jan, V.; Dlouhy, I. Characterization of powder metallurgy high-entropy alloys prepared by spark plasma sintering. In *Materials Science Forum*; Trans Tech Publication Ltd.: Cham, Switzerland, 2018; Volume 941, pp. 1053–1058, ISBN 9783035712087.
11. Waseem, O.A.; Ryu, H.J. Powder Metallurgy Processing of a W(x)TaTiVCr High-Entropy Alloy and Its Derivative Alloys for Fusion Material Applications. *Sci. Rep.* **2017**, *7*, 1926. [CrossRef]
12. Löbel, M.; Lindner, T.; Lampke, T. Enhanced Wear Behaviour of Spark Plasma Sintered AlCoCrFeNiTi High-Entropy Alloy Composites. *Materials* **2018**, *11*, 2225. [CrossRef]
13. Cantor, B.; Chang, I.T.H.; Knight, P.; Vincent, A.J.B. Microstructural development in equiatomic multicomponent alloys. *Mater. Sci. Eng. A* **2004**, *375–377*, 213–218. [CrossRef]
14. Yeh, J.W.; Chen, S.K.; Lin, S.J.; Gan, J.Y.; Chin, T.S.; Shun, T.T.; Tsau, C.H.; Chang, S.Y. Nanostructured High-Entropy Alloys with Multiple Principal Elements: Novel Alloy Design Concepts and Outcomes. *Adv. Eng. Mater.* **2004**, *6*, 299–303. [CrossRef]

15. Gludovatz, B.; Hohenwarter, A.; Catoor, D.; Chang, E.H.; George, E.P.; Ritchie, R.O. A fracture-resistant high-entropy alloy for cryogenic applications. *Science* **2014**, *345*, 1153–1158. [CrossRef] [PubMed]
16. Senkov, O.N.; Miracle, D.B.; Chaput, K.J.; Couzinie, J.-P. Development and exploration of refractory high entropy alloys—A review. *J. Mater. Res.* **2018**, *33*, 3092–3128. [CrossRef]
17. Moravcik, I.; Hadraba, H.; Li, L.; Dlouhy, I.; Raabe, D.; Li, Z. Yield strength increase of a CoCrNi medium entropy alloy by interstitial nitrogen doping at maintained ductility. *Scr. Mater.* **2020**, *178*, 391–397. [CrossRef]
18. Li, Z.; Pradeep, K.G.; Deng, Y.; Raabe, D.; Tasan, C.C. Metastable high-entropy dual-phase alloys overcome the strength–ductility trade-off. *Nature* **2016**, *534*, 227–230. [CrossRef]
19. Su, J.; Raabe, D.; Li, Z. Hierarchical microstructure design to tune the mechanical behavior of an interstitial TRIP-TWIP high-entropy alloy. *Acta Mater.* **2019**, *163*, 40–54. [CrossRef]
20. Gludovatz, B.; Hohenwarter, A.; Thurston, K.V.S.; Bei, H.; Wu, Z.; George, E.P.; Ritchie, R.O. Exceptional damage-tolerance of a medium-entropy alloy CrCoNi at cryogenic temperatures. *Nat. Commun.* **2016**, *7*, 10602. [CrossRef]
21. Praveen, S.; Kim, H.S. High-Entropy Alloys: Potential Candidates for High-Temperature Applications—An Overview. *Adv. Eng. Mater.* **2018**, *20*, 1700645. [CrossRef]
22. Moravcik, I.; Hornik, V.; Minárik, P.; Li, L.; Dlouhy, I.; Janovska, M.; Raabe, D.; Li, Z. Interstitial doping enhances the strength-ductility synergy in a CoCrNi medium entropy alloy. *Mater. Sci. Eng. A* **2020**, *781*, 139242. [CrossRef]
23. Vaidya, M.; Karati, A.; Marshal, A.; Pradeep, K.G.; Murty, B.S. Phase evolution and stability of nanocrystalline CoCrFeNi and CoCrFeMnNi high entropy alloys. *J. Alloys Compd.* **2019**, *770*, 1004–1015. [CrossRef]
24. Hryha, E.; Shvab, R.; Bram, M.; Bitzer, M.; Nyborg, L. Surface chemical state of Ti powders and its alloys: Effect of storage conditions and alloy composition. *Appl. Surf. Sci.* **2016**, *388*, 294–303. [CrossRef]
25. Li, J.; Yu, J.; Li, W.; Che, S.; Zheng, J.; Qiao, L.; Ying, Y. The preparation and magnetic performance of the iron-based soft magnetic composites with the Fe@Fe3O4 powder of in situ surface oxidation. *J. Magn. Magn. Mater.* **2018**, *454*, 103–109. [CrossRef]
26. Deffley, R. *Vacuum vs. Non-Vacuum Melted Gas Atomized Powders*; Carpenter technology: Philadelphia, PA, USA, 2017.
27. Mújica Roncery, L.; Weber, S.; Theisen, W. Nucleation and precipitation kinetics of M23C6 and M2N in an Fe–Mn–Cr–C–N austenitic matrix and their relationship with the sensitization phenomenon. *Acta Mater.* **2011**, *59*, 6275–6286. [CrossRef]
28. Luo, X.-T.; Li, C.-J.; Yang, G.-J. Correlations between milling conditions and iron contamination, microstructure and hardness of mechanically alloyed cubic BN particle reinforced NiCrAl matrix composite powders. *J. Alloys Compd.* **2013**, *548*, 180–187. [CrossRef]
29. Fernandes, B.B.; Rodrigues, G.; Coelho, G.C.; Ramos, A.S. On iron contamination in mechanically alloyed Cr–Si powders. *Mater. Sci. Eng. A* **2005**, *405*, 135–139. [CrossRef]
30. Castle, E.; Csanádi, T.; Grasso, S.; Dusza, J.; Reece, M. Processing and Properties of High-Entropy Ultra-High Temperature Carbides. *Sci. Rep.* **2018**, *8*, 8609. [CrossRef]
31. Le Claire, J.J.; Laitila, E.A.; Mikkola, D.E. Forming nanostructured cubic trialuminide/carbide composites by mechanical milling followed by thermal processing. *Scr. Mater.* **2004**, *50*, 95–98. [CrossRef]
32. Mackie, A.J.; Hatton, G.D.; Hamilton, H.G.C.; Dean, J.S.; Goodall, R. Carbon uptake and distribution in Spark Plasma Sintering (SPS) processed Sm(Co, Fe, Cu, Zr)z. *Mater. Lett.* **2016**, *171*, 14–17. [CrossRef]
33. Takeuchi, A.; Inoue, A. Classification of Bulk Metallic Glasses by Atomic Size Difference, Heat of Mixing and Period of Constituent Elements and Its Application to Characterization of the Main Alloying Element. *Mater. Trans.* **2005**, *46*, 2817–2829. [CrossRef]